A Diffraction Transfer Function Approach to the Calculation of the Transient Field of Acoustic Radiators

Chankil Lee

CONTENTS

ABSTRACT

A computationally-efficient approach to the calculation of the transient field of an acoustic radiator was developed. With this approach, a planar or curved source, radiating either continuous or pulsed waves, is divided into a finite number of shifted and/or rotated versions of an incremental source such that the Fraunhofer approximation holds at each field point. The acoustic field from the incremental source is given by a 2-D spatial Fourier transform. The diffraction transfer function of the entire source can be expressed as a sum of Fraunhofer diffraction pattern of the incremental sources with the appropriate coordinate transformations for the particular geometry of the radiator. For a given spectrum of radiator velocity, the transient field can be computed directly in the frequency domain using the diffraction transfer function. To determine the accuracy of the proposed approach, the impulse response was derived using the inverse Fourier transform. The results obtained agree well with published data obtained using the impulse response approach. The computational efficiency of the proposed method compares favorably to those of the point source method and the impulse response approach.

I. INTRODUCTION

The calculation of the transient acoustic field produced by an ultrasonic transducer has been the subject of numerous investigations for the past two decades. To date, the most efficient analytic tool for this calculation on uniformly vibrating pistons is the impulse response approach by Stepanishen [1,2]. This approach has also been applied to the case of nonuniform axisymmetric vibrating pistons [3-5]. For both of these cases the acoustic transient field was related to the derivative of the radiating source velocity waveform by means of temporal convolution with an impulse response function. This function took into account the geometrical shape of the vibrating surface, the position in space of the observation point. The spatial impulse response, as a function of time for a fixed field point, has been determined in closed form for circular pistons [6], rectangular sources [7], conical radiators [8], and for spherical sources [9-11].

To calculate the acoustic transient field, an integral computation, which can be evaluated either numerically [6,9] or by means of a fast Fourier transform (FFT) algorithm [2], is required for each data point in the field. In either case, it is necessary to sample the functions involved in the convolution in order to perform the numerical integration. Unfortunately, the discontinuities and break-point characteristics of the impulse response complicate this procedure. Moreover, the field calculation is more intensive in the case of an arbitrary excitation, especially when the amplitude is not an analytic function [12]. To reduce the operations involved in the convolutional integral, the monodimensional radiating surface can be expressed as a sum of small elements so that the impulse response is simply given by the sum of delta functions properly time shifted and weighted [13]. However, in order to derive the impulse response for arbitrary shaped radiators, a laborious procedure resorting to geometric interpretation is necessary. In many cases, the off-axis impulse response for such radiators is not amendable to an analytic solution, and thus must be computed by numerical methods [8]. In addition, this approach is not readily adaptable to consider the effects due to attenuation and dispersion of the propagating medium on radiating fields.

Among other approaches developed for acoustic field calculations, one of the more notable is based on Huygens' principle and uses a double numerical integration of the Rayleigh-Sommerfeld diffraction integral. For the numerical integration, the surface of the radiator was divided into incremental point sources for a circular piston [14]. The total field is then expressed as a sum of each contributions, spherical wavefront, from the point sources. To obey the sampling theorem in the temporal and spatial domains, the size of the incremental point source should be at most $(\lambda/4)^2$ for the farfield and even smaller for nearfield (λ=wavelength of sound in the propagating medium). Thus,

even with this approximation, this approach is still computationally intensive due to the large number of point sources. With an assumption of a sine-modulated Gaussian pulsed excitation, this approach was applied to calculate the transient field from various shapes of radiators [15,16], with some loss in accuracy for the case of curved radiators because the normal directions of the particle velocity on the radiating surface are not identical, and attenuating media [17].

In this paper, a computationally efficient method, the diffraction transfer function approach, similar to the space linear system approach of Fourier optics [18], to an analysis of wideband diffraction problems using the spatial Fourier transform and coordinates transformations is proposed. This approach can be applied to any shape of radiator driven by continuous wave (CW) or pulsed excitations. Both amplitude and time-delay control, as well as nonuniform spatial efficiencies, can easily be considered with this approach. Quantitative comparisons of the computational efficiency and accuracy of the proposed method with the point source method and the impulse response approach are made to demonstrate its advantages.

II. THEORY

For any plane piston radiator of area S surrounded by an infinite plane rigid baffle in an unbounded fluid, the velocity potential at the observation point $\mathbf{r}$ is given by [19]

$$\phi(\mathbf{r},t)=\frac{1}{2\pi}\int_S \frac{v_n(\mathbf{r}_S,t-r/c)}{r}dS, \qquad (1)$$

where $r=|\mathbf{r}-\mathbf{r}_S|$ is the distance between the field point $\mathbf{r}$ and the source point $\mathbf{r}_S$. The velocity of the piston, $v_n(\cdot)$, in the direction normal to the source plane is given by

$$v_n(\mathbf{r}_S,t)=v_0(t)s(x,y), \qquad (2)$$

where the time dependence, $v_0(t)$, is a function of the input signal and electromechanical properties of the transducer, while the spatial function, $s(x,y)$, depends on the sensitivity and geometrical shape of the radiator.

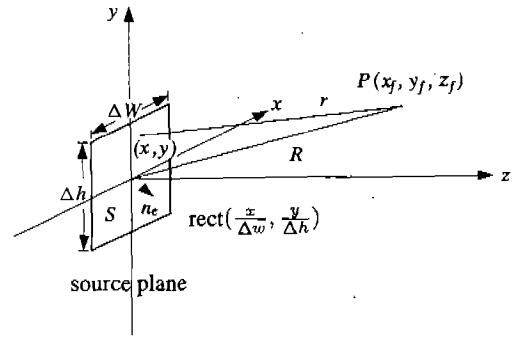

Fig. 1. The geometry for the diffraction calculation from a rectangular source.

To calculate the surface integral, the radiating surface is divided into a number of incremental sources which are too large to be represented as point sources but small enough so that at the field point $\mathbf{r}$, the computationally efficient Fraunhofer diffraction approximation can be applied. Fig. 1 shows the geometry for

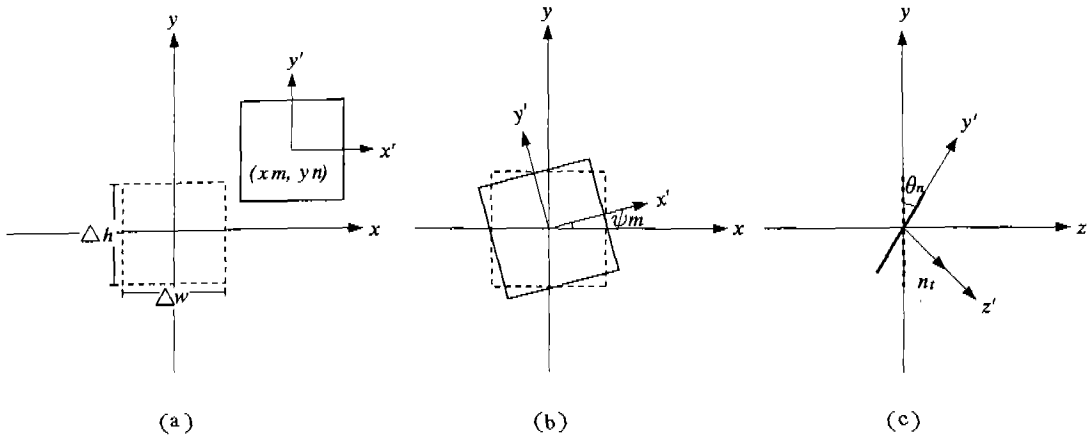

Fig. 2. Coordinate transformations used for field calculations (a) shift, (b) $x-y$ rotation, (c) $y-z$ rotation.

the diffraction calculation from an incremental source centered at the origin of the coordinates axes. Since $z \leq R$, the width, Δw, and height, Δh, of the incremental source which satisfy the far-field condition are given by

$$\Delta w, \Delta h \leq \sqrt{4\lambda z/F}, \tag{3}$$

where λ is the wavelength and the constant F represents the distance from the source to the field point relative to the distance to the near-far field transition for a source of size Δw, Δh [20]. Thus, the size of the incremental source is determined by the radiated wavelength and the z distance of the field point. As F becomes large, the incremental source looks more like a point source.

The radiator surface can be constructed with incremental sources which are shifted and/or rotated versions of the source in Fig. 1. The old and new coordinates are (x, y, z) and (x', y', z'), respectively. Fig. 2(a) shows the shift of an incremental source to (x_m, y_n). The shift operator can be expressed by the delta function defined by

$$\delta(x-x_m, y-y_n) = \begin{cases} 1, & \text{if } (x, y) = (x_m, y_m) \\ 0, & \text{otherwise.} \end{cases} \tag{4}$$

To describe a rotation, as illustrated in Fig. 2(b), cylindrical coordinates are used. In this example, the incremental source is rotated through a positive (counter-clockwise) angle of ψ_m. The x-y rotation operator is given by

$$R_{\psi_m} = \begin{bmatrix} \sin\psi_m & \cos\psi_m & 0 \\ -\cos\psi_m & \sin\psi_m & 0 \\ 0 & 0 & 1 \end{bmatrix}. \tag{5}$$

For curved axisymmetric radiators, an additional rotation, as shown in Fig. 2(c), is nec-

essary due to the 3-D geometry of the radiator surface. The y-z rotation operator is given by

$$R_{\theta_n} = \begin{bmatrix} 1 & 0 & 0 \\ 0 & \cos\theta_n & -\sin\theta_n \\ 0 & \sin\theta_n & \cos\theta_n \end{bmatrix}. \quad (6)$$

The normal vector at the center of the transformed incremental source, $\mathbf{n}_t$, can be expressed using the rotation operation on the normal vector, $\mathbf{n}_e$, of the incremental source as

$$\begin{aligned} \mathbf{n}_t &= R_{\psi_m}\{R_{\theta_n}\{\mathbf{n}_e\}\} \\ &= -\sin\theta_n(\cos\psi_m\mathbf{x} + \sin\psi_m\mathbf{y}) \\ &\quad + \cos\theta_n\mathbf{z}, \end{aligned} \quad (7)$$

where $0 \le \psi_m < 2\pi$ for axisymmetric radiators and θ_n depends on the curvature function of radiator. For the planar radiators, $\theta_n = 0$, $\mathbf{n}_t = \mathbf{z}$.

1. Continuous Excitation

A time-independent expression of the velocity potential of Eq. (1) for a sinusoidal field reduces to

$$\Phi(\mathbf{r}) = \frac{v_\circ}{2\pi}\int_S s(x,y)\frac{e^{-(\alpha+jk)r}}{r}dxdy, \quad (8)$$

where $k(\omega) = \omega/c(\omega)$ is the wave number, $\alpha(\omega)$ is the attenuation coefficient, and $v_\circ$ is the complex velocity amplitude. If the incremental source is an uniform rectangular source, then

$$s(x,y) = \mathrm{rect}(\frac{x}{\Delta w}, \frac{y}{\Delta h}). \quad (9)$$

To find an expression for the acoustic field which can be easily evaluated numerically, suitable approximations and their regions of applicability must be defined. In the far-field region where the condition of Eq. (3) is satisfied, the omission of second and higher order terms of a binomial expansion of r produces a negligible phase error and yields

$$e^{-(\alpha+jk)r} \simeq e^{(\alpha+jk)[R-\frac{x_f x}{R}-\frac{y_f y}{R}]}, \quad (10)$$

where $R = \sqrt{x_f^2 + y_f^2 + z_f^2}$. Using this approximation and assuming $1/r \simeq 1/R$, Eq. (8) becomes

$$\begin{aligned} \Phi_\circ(\mathbf{r}) = \frac{v_\circ e^{-(\alpha+jk)R}}{2\pi R}&\int_{-\Delta w/2}^{\Delta w/2} e^{(\alpha+jk)\frac{x_f x}{R}}dx \\ &\times \int_{-\Delta h/2}^{\Delta h/2} e^{(\alpha+jk)\frac{y_f y}{R}}dy. \end{aligned} \quad (11)$$

The assumption that $e^{\alpha x_f \Delta w/2R} \simeq 1$ and the equivalent condition for y are used to simplify the two integrals. The velocity potential from an incremental source can now be expressed by its 2-D spatial Fourier transform

$$\begin{aligned} \Phi_\circ(\mathbf{r}) &= \frac{v_\circ e^{-(\alpha+jk)R}}{2\pi R}\mathcal{F}\{\mathrm{rect}(\frac{x}{\Delta w}, \frac{y}{\Delta h})\} \\ &\quad | f_x = \frac{x_f}{\lambda R}, f_y = \frac{y_f}{\lambda R} \\ &= \frac{v_\circ \Delta A e^{-(\alpha+jk)R}}{2\pi R}\mathrm{sinc}(\frac{\Delta w x_f}{\lambda R}) \\ &\quad \times \mathrm{sinc}(\frac{\Delta h y_f}{\lambda R}), \end{aligned} \quad (12)$$

where f_x and f_y are the spatial frequencies in the x and y dimensions, respectively. This simple Fourier expression is used as a basis

function for synthesizing the total field pattern. The total velocity potential Φ at a point $\mathbf{r}$ in the field is the sum of the pressure contributed from each incremental source

$$\Phi(x, y, z) = \sum_{n=0}^{N-1} \sum_{m=0}^{M-1} \Phi_0(x', y', z'), \quad (13)$$

where MN is the number of incremental sources of size $\Delta A = \Delta w \Delta h$. The necessary transformations for the evaluation of Φ_0 at each incremental sources are the transpose operators which give the normal vector of the elementary source

$$\tilde{R}_{\theta_n}\{\tilde{R}_{\psi_m}\{\mathbf{n}_t\}\} = \mathbf{n}_e. \quad (14)$$

2. Pulsed Excitation

For a pulsed excitation, the spatial impulse response has been used to compute the field [1,3-13]. The following analysis is based on a frequency domain approach using the transfer function of the impulse response [2]. The convolution integral can be evaluated directly in the frequency domain to obtain the time dependent pressure. The instantaneous velocity potential at a point in the frequency domain can be written as

$$\Phi(\mathbf{r}, \omega) = V(\omega) H(\mathbf{r}, \omega), \quad (15)$$

where $V(\omega)$ is the spectrum of the excitation signal $v_0(t)$ in Eq. (2), and $H(\mathbf{r}, \omega)$, the diffraction transfer function, is the Fourier transform of the impulse response, $h(\mathbf{r}, t)$. The pressure in the frequency domain is the diffraction transfer function, developed in Eq. (13), weighted by the spectral shape of radiator velocity,

$$\begin{aligned} P(\mathbf{r}, \omega) &= j\rho\omega\Phi(\mathbf{r}, \omega) \\ &= j\rho\omega V(\omega) H(\mathbf{r}, \omega). \end{aligned} \quad (16)$$

Thus, if $H(\mathbf{r}, \omega)$ is computed at every harmonic frequency, $\omega_k = 2\pi k/L$, where L is the number of decomposed harmonic frequencies, the Fourier transform of the pressure field for a pulse-excited source can be found. The evaluation of $H(\mathbf{r}, \omega)$ can be simplified if only those portions of the radiator spectrum within 3-dB or 6-dB of the fundamental are considered for the synthesis of $P(\mathbf{r}, \omega)$. The instantaneous field pressure is given by the inverse Fourier transform,

$$p(\mathbf{r}, t) = \mathcal{F}^{-1}\{P(\mathbf{r}, \omega)\}. \quad (17)$$

As shown in Eq. (3), the size of the incremental source varies only with the z field position for the CW excitation. However, for the pulsed excitation, the size of the incremental source depends both on the wavelength and z position of the field point

$$\Delta w, \Delta h \leq \sqrt{\frac{4\lambda_k z}{F}}, \quad (18)$$

where $\lambda_k = 2\pi c/\omega_k$. Therefore, the the number of harmonic frequencies included in the evaluation of the diffraction transfer function and F control the trade-off between the computational efficiency and accuracy.

For medical ultrasonic imaging and nonde structive testing, theattenuation of the radiation field and resulting shift in phase velocity are

important features. The influence of attenuation and dispersion in the propagating medium on the radiation field can be considered by including the complex wave number **k** into Eq. (12),

$$\begin{aligned}\mathbf{k}(\omega) &= k(\omega) - j\alpha(\omega) \\ &= \omega/c(\omega) - j\alpha(\omega), \end{aligned} \tag{19}$$

where $\alpha(\omega)$ is the frequency dependent attenuation coefficient and (ω) is the phase velocity of the propagating medium.

III. SOURCE GEOMETRY EXAMPLES

1. Planar Radiators

A. *Rectangular Sources*

The rectangular radiator of width $2a$ and height $2b$, shown in Fig. 3(a), is given by a finite number of shifted incremental sources

$$\begin{aligned} s(\mathbf{r}_S) &= \mathrm{rect}\left(\frac{x}{\Delta w}, \frac{y}{\Delta h}\right) \\ &\quad ** \sum_{n=0}^{N-1} \sum_{m=0}^{M-1} \delta(x - x_m, y - y_n), \end{aligned} \tag{20}$$

where the numbers of divisions are

$$M = 2a/\Delta w, \qquad N = 2b/\Delta h,$$

where Δw and Δh are chosen to satisfy Eq. (3) and yield integer values for M and N. The center of an incremental source is expressed by

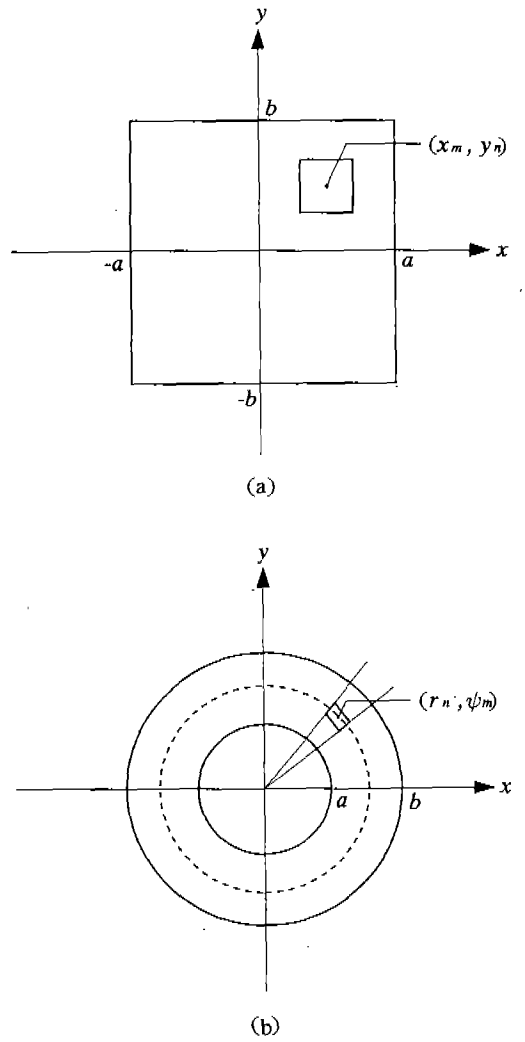

Fig. 3. Geometry used for calculation of an acoustic field from planar radiators. (a) rectangular, (b) circular.

$$x_m = -a + (m + 0.5)\Delta w,$$

$$y_n = -b + (n + 0.5)\Delta h$$

and the field points in the new coordinates are given by

$$x' = x_f - x_m,$$
$$y' = y_f - y_n,$$
$$z' = z_f. \tag{21}$$

A similar expression was used by Ocheltree and Frizzell for the field calculation of a rectangular source [20]. This method can be easily adapted to any shape of planar linear array transducer by modifying Eq. (2).

B. *Circular Sources*

Cylindrical coordinates are used to describe planar axisymmetric radiators. An annular radiator with inner radius a and outer radius b, as shown in Fig. 3(b), can be approximated by a finite number of shifted and rotated incremental sources

$$s(\mathbf{r}_S) = \sum_{n=0}^{N-1}\sum_{m=0}^{M-1} R_{\psi_m}\{\mathrm{rect}(\frac{x}{\Delta w}, \frac{y}{\Delta h})\} \\ **\delta(r - r_n, \psi - \psi_m), \tag{22}$$

where the integer numbers of divisions are

$$M = 2\pi r_n/\Delta w,$$
$$N = (b-a)/\Delta h.$$

The center of an incremental source is expressed by

$$r_n = a + (n+0.5)\Delta h,$$
$$\psi_m = (m+0.5)\Delta w/r_n$$

and the field points in the new coordinates are given by

$$\begin{bmatrix} x' \\ y' \\ z' \end{bmatrix} = \tilde{R}_{\psi_m} \cdot \begin{bmatrix} x_f - r_n\cos\psi_m \\ y_f - r_n\sin\psi_m \\ z_f \end{bmatrix} \tag{23}$$

This method can be easily adapted to any shape of planar axisymmetric radiator including an annular array.

2. Curved Radiators

Only conical and spherical surfaces will be considered here, but this approach can be applied to any shape of curved axisymmetric radiators [21]. Using cylindrical coordinates, an axisymmetric curved radiator can be approximated by a finite number of shifted and rotated incremental sources as

$$s(\mathbf{r}_S) = \sum_{n=0}^{N-1}\sum_{m=0}^{M-1} R_{\psi_m}\{R_{\theta_n}\{\mathrm{rect}(\frac{x}{\Delta w}, \frac{y}{\Delta h})\}\} \\ ***\delta(r - r_n, \psi - \psi_m, z - z_n). \tag{24}$$

For the case of a curved radiator, it is assumed that the surface of the radiator is only slightly curved, where the diameter of the radiator is large compared to the wavelength and the radiator depth, so that the secondary diffraction caused by the curvature of the radiator is negligible [5,11]. Thus, the velocity potential can be represented approximately by the Rayleigh integral.

A. *Conical Radiators*

A conical radiator of angle $\theta_n = \theta$, with inner

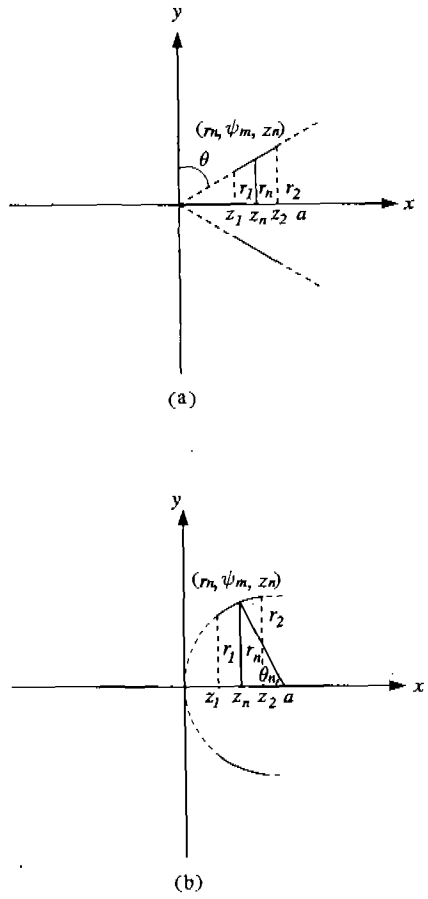

Fig. 4. Geometry used for calculation of the acoustic fields from curved axisymetric radiators. (a) conical, (b) spherical radiator.

and outer radii r_1 and r_2, is shown in cross section in Fig. 4(a). Eq. (3) can not be used directly, due to the 3-D shape of the radiator, to determine the size of the incremental source. Therefore, z in Eq. (3) is replaced by l which is the minimum distance between the field points and the radiator surface. This substitution yields

$$M = 2\pi r_n / \Delta w,$$
$$N = (z_2 - z_1)/(\sin\theta \Delta h).$$

The center of an incremental source is expressed by

$$r_n = \frac{z_n}{\tan\theta},$$
$$\psi_m = \frac{(m+0.5)\Delta w}{r_n},$$
$$z_n = z_1 + (n+0.5)\Delta h \sin\theta,$$

and the field points in the new coordinates are given by

$$\begin{bmatrix} x' \\ y' \\ z' \end{bmatrix} = \tilde{R}_{\theta_n} \tilde{R}_{\psi_m} \cdot \begin{bmatrix} x_f - r_n \cos\psi_m \\ y_f - r_n \sin\psi_m \\ z_f - z_n \end{bmatrix}. \quad (25)$$

B. *Spherical Radiator*

A spherical radiator with a radius of curvature a, and inner and outer radii r_1 and r_2, is shown in cross section in Fig. 4(b). The numbers of divisions for this case are determined in the same manner as for the conical radiator. Thus, M and N are given by

$$M = 2\pi r_n / \Delta w,$$
$$N = a(\cos^{-1}((a - z_2)/a) - \cos^{-1}((a - z_1)/a))/\Delta h.$$

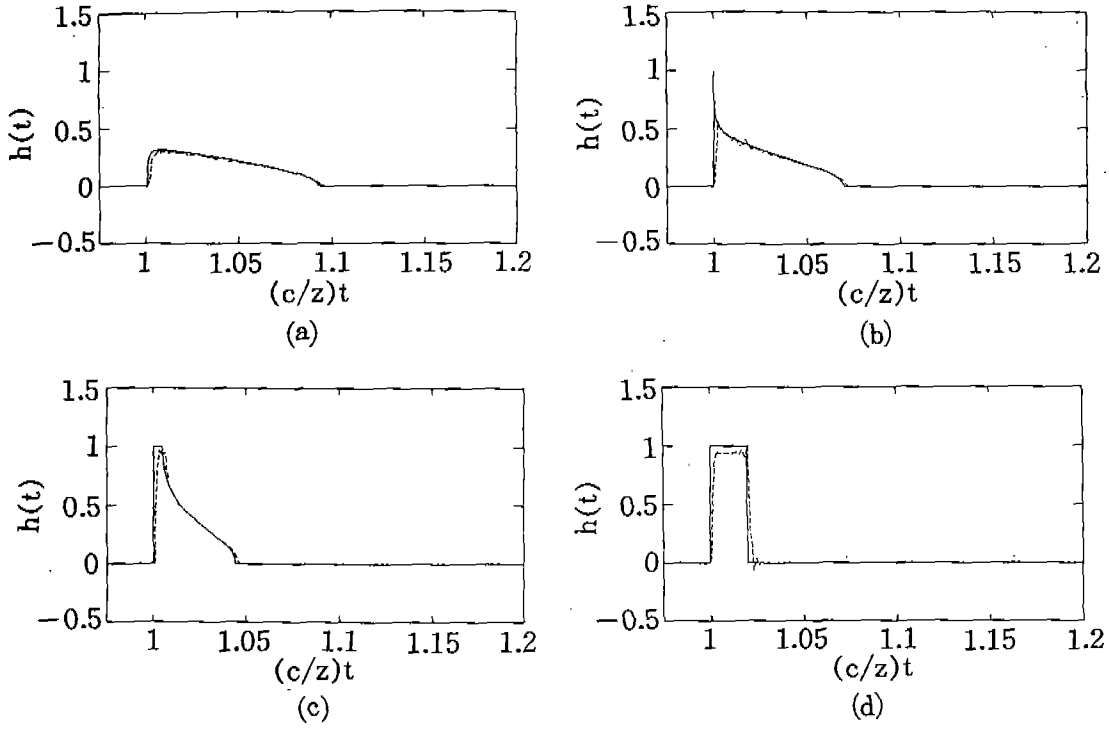

Fig. 5. Impulse response of a circular piston radiator ($a=0, z/b=5$), for several off-axis distances r, as a function of normalized time. Impulse response approach (solid) and diffraction transfer function approach (dashed) curves. (a) $r/a=1.2$, (b) $r/a=0.9$, (c) $r/a=0.5$, (d) $r/a=0.0$.

The center of an incremental source is expressed by

$$r_n = a\sin\theta_n,$$
$$\psi_m = \frac{(m+0.5)\Delta w}{r_n},$$
$$z_n = a(1-\cos\theta_n),$$
$$\theta_n = \cos^{-1}((a-z_1)/a) + \frac{(n+0.5)\Delta h}{a}$$

and the field points in the new coordinates are given by Eq. (23).

IV. SIMULATION RESULTS AND DISCUSSION

To determine the accuracy of the transient fields obtained with the proposed approach, a direct comparison can be made with published results obtained using the impulse response approach. To accomplish this, $V(\omega_k)$ is set equal to unity in Eq. (14) and sampled at $\omega_k = 2\pi f_s k/L, k=0,1,\cdots,L/2$, where f_s is the sampling frequency. For an L-point real

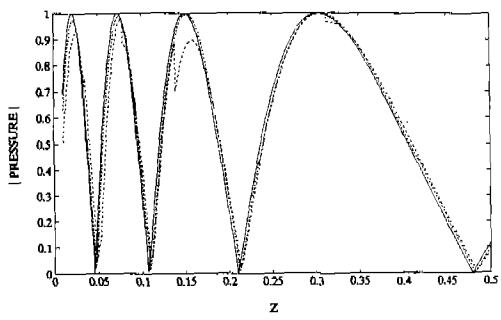

Fig. 6. Normalized on-axis response of a circular piston radiator ($a=0, b=5\lambda$) as a function of normalized axial distance $Z=z\lambda/b^2$. (solid: exact solution; dashed: F=15; dotted: F=10; dashdot: F=5)

sequence, the Fourier transform is conjugate symmetric, where

$$H(k)=H^*(L-k), \quad k=1,\cdots,L/2-1. \tag{26}$$

The resulting inverse FFT of $H(k)$ yields a finite duration sequence as one period of circular periodic sequence, $\tilde{h}$, with the duration of period $T=L/f_s$. This sequence can be expressed as

$$h(\mathbf{r},n)=\begin{cases}\tilde{h}(\mathbf{r},n), & 0\le n<L\\ 0, & \text{otherwise}\end{cases} \tag{27}$$

where

$$\tilde{h}(\mathbf{r},n)=\sum_{q=-\infty}^{\infty} h(\mathbf{r},n+qL).$$

Unfortunately, the discontinuities and breakpoint characteristics of $h(\mathbf{r},t)$ complicate this procedure. This problem is particularly severe for field points close to the boundary of the geometric projection of the source. Therefore, the sampling rate f_s should be high enough to approximate this sudden slope. If the duration of the impulse response is greater than T, there will be overlap of nonzero samples, resulting in aliasing. Thus, L/f_s should be chosen large enough to avoid aliasing for the calculation of the impulse response.

The impulse response of a circular piston radiator is computed and compared directly with the exact solutions obtained with the impulse response approach in Fig. 5. The source geometry and field point are the same as those considered by Lockwood and Willette [6]. For this simulation, $F=10$, $f_s=100$ MHz and $L=1024$. This figure demonstrates that good agreement is achieved with the exact solution. To consider the effect of F on the accuracy of the proposed method, the normalized axial pressure for a circular piston radiator with radius $b=5\lambda$ was calculated and compared with the exact solution. Fig. 6 shows that the amplitude and location of the minimum and maximum match well with the exact solution for F≥10.

The impulse responses with a proposed method were also computed for rectangular, conical, and spherical radiators in Figs. 7, 8, and 9, respectively. For the cases of curved axisymmetric radiators, f_s = 100 MHz and

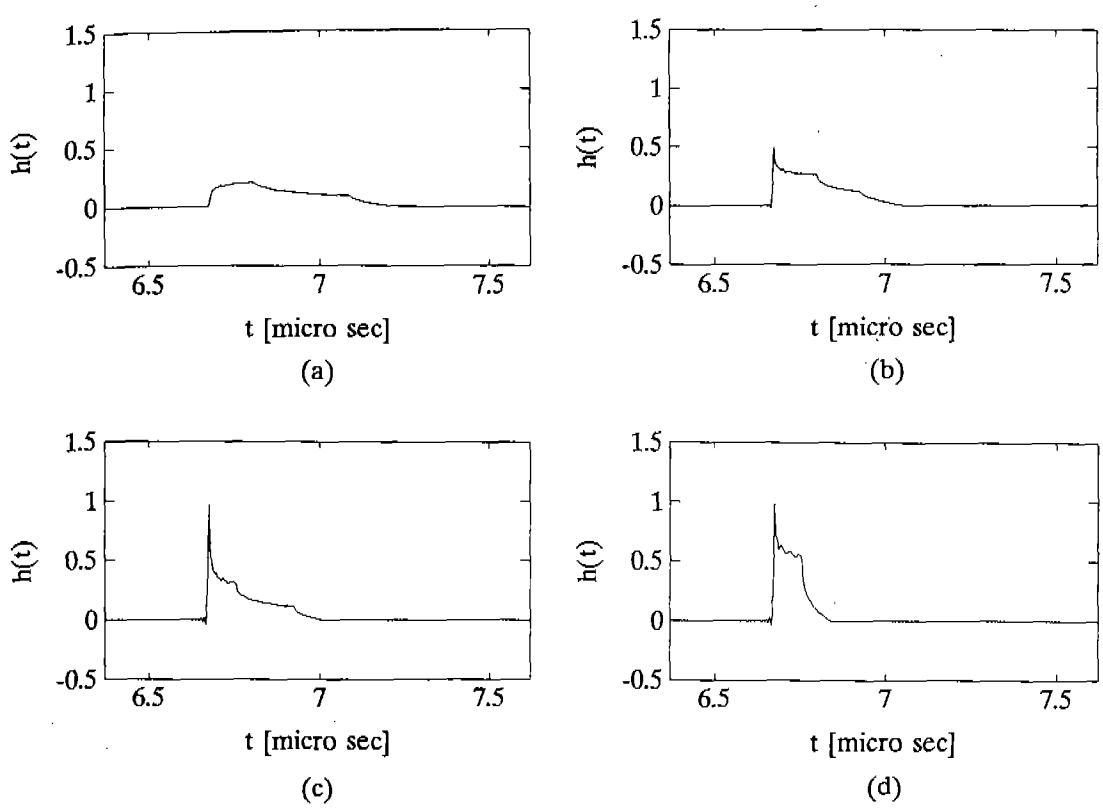

Fig. 7. Impulse response of a rectangular piston radiator ($a=1$mm, $b=1.6$mm), for $z=10.0$mm, as a function of time. (a) $x=1.0$, $y=2.0$, (b) $x=1.0$, $y=1.2$, (c) $x=0.6$, $y=1.2$, (d) $x=0.6$, $y=0.0$.

$L=2048$ points were used. Comparing these results to those obtained with impulse response approaches [7,8,11] again revealed that good agreement is obtained.

To make an estimate of the computational efficiency of the proposed method relative to those of the point source method and impulse response approach, a circular piston radiator radius of a is considered. The efficiency of the proposed approach is greater than that of the point source method by a factor equivalent to the ratio of the number of point sources to the number of incremental sources in a radiator. As the distance from the radiator increases, the number of incremental sources required will decrease by virtue of the relationship of Eq. (3). In the point source method [14], the required number of divisions was $(\pi a^2)/(\lambda/4)^2$ to attain a convergent field. In the proposed method, the number of divisions is given by $(\pi a^2)/(4\lambda z/F)$. Thus, for $F=10$, the efficiency of the proposed approach is

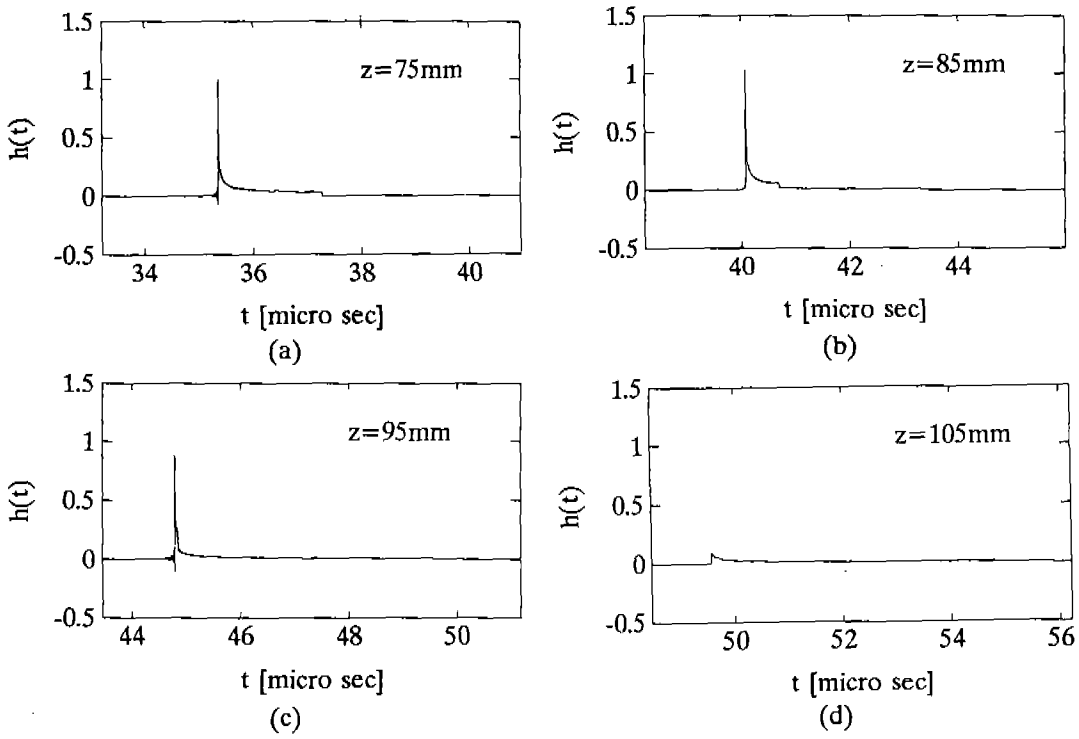

Fig. 8. Impulse response of a 45° conical radiator ($z_1 = 25$ mm, $z_2 = 50$ mm) as a function of time. (a)-(d) on the axis.

greater than the point source method over the region of $z > \lambda/6$. The impulse response approach requires the sampling of the impulse response in the time domain and a temporal convolution. The high-speed method proposed by Lockwood and Willette [6], used a sampling rate of 10 times per cycle of the driving frequency for a convergent field. Because the maximum length of the nonconstant part of the impulse response is $2a/c$, the upper bound on the number of calculations in that method is $10f \cdot 2a/c$. Thus, the number of calculations is proportional to a/λ, whereas that of the proposed method is proportional to $a^2/\lambda z$. Therefore, a rough approximation indicates the proposed method is more efficient than the Lockwood and Willette method over the region $z > a/20$ for CW excitations and $z > B \cdot L/f_s \cdot a/20$ for pulsed excitations, where B [MHz] is the bandwidth of a radiator employed in the computation. This implies that a computationally efficient region of the proposed method decreases as $B, L/f_s$, and a increases.

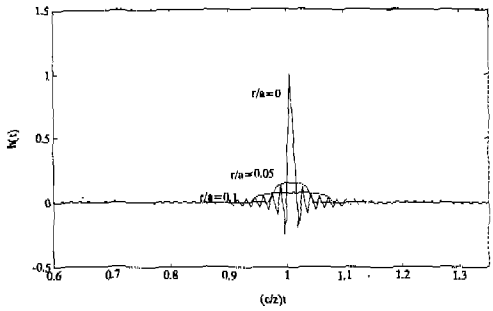

Fig. 9. Impulse response of a spherical radiator ($r_1 = 0, r_2/a = 1/\sqrt{2}$) as a function of normalized time at $z = a$ field point.

V. CONCLUSION

The diffraction integral for arbitrary shaped radiators can be computed using a spatial Fourier transform approach and coordinate transformations. The diffraction transfer function derived using this approach provides a simple and accurate computational expression for the calculation of the transient field. In addition, this approach is applicable to both CW and pulsed excitations for any radiator geometry where the exact closed-form solution for the impulse response can not be derived and is readily adaptable to consider either the effects due to attenuation and dispersion of the propagating medium on radiating fields or the radiation from secondary sources such as an acoustic lens/mirror.

The simulation results show that $F = 10$ was sufficient to attain the convergent field which matches well with those obtained with the impulse response approach for both planar and axisymmetric curved radiators. The relative computational efficiency of the proposed method compares favorably to those of the point source method and the impulse response approach.

ACKNOWLEDGEMENT

The author wishes to express special thanks to his advisor Paul J. Benkeser at Goergia Tech for valuable discussions and supporting the work.

REFERENCES

[1] P. R. Stepanishen, "Transient Radiation from Pistons in an Infinite Planar Baffle," *J. Acoust. Soc. Am.*, vol.49, no.5, pp.1629-1637, 1970.

[2] P. R. Stepanishen, "Wide Bandwidth Acoustic Near and Far Field Transients from Baffled Pistons," *IEEE Ultrasonic Symp. Proc.*, pp.113-118, 1977.

[3] P. R. Stepanishen, "Acoustic Transients from Planar Axisymmetric Vibrators Using the Impulse Response Approach," *J. Acoust. Soc. Am.*, vol.70, no.4, pp.1176-1181, 1981.

[4] G. R. Harris, "Review of Transient Field Theory for a Baffled Planar Piston," *J. Acoust. Soc. Am.*, vol.70, no.1, pp.10-20, 1981.

[5] J. N. Tjϕtta and S. Tjϕtta, "Nearfield and Farfield of Pulsed Acoustic Radiators," *J. Acoust. Soc. Am.*, vol.71, no.4, pp.824-834, 1982.

[6] J. C. Lockwood and J. G. Willette, "High-Speed Method for Computing the Exact Solution for the Pressure Vibrations in the Nearfield of a Baffled Pistion," *J. Acoust. Soc. Am.*, vol.53, no.3, pp.735-

741, 1972.

[7] G. Scarano, N. Denisenko, M. Matteucci and M. Pappalardo, "A New Approach to the Derivation of the Impulse Response of a Rectangular Piston," *J. Acoust. Soc. Am.*, vol.78, no.3, pp.1109-1113, 1985.

[8] M. S. Patterson and F. S. Foster, "Acoustic Fields of Conical Radiators," *IEEE Trans. Son. Ultrason.*, vol.SU-29, no.2, pp.83-92, 1982.

[9] M. Arditi, F. S. Forster and J. W. Hunt, "Transient Fields of Concave Annular Arrays," *Ultrasonic Imaging*, no.3, pp.37-61, 1981.

[10] W. A. Verhoef, M.J.T.M. Cloostermans and J. M. Thijssen, "The Impulse Response of a Focused Source with an Arbitrary Axisymmetric Surface Velocity Distribution," *J. Acoust. Soc. Am.*, vol.75, no.6, pp.1716-1721, 1984.

[11] A. Penttinen and M. Luukkala, "The Impulse Response and Pressure Nearfield of a Curved Ultrasonic Radiator," *J. Phys. D: Appl. Phys.*, no.9, pp.1547-1557, 1976.

[12] H. Lasota, R. Salamon, and Delannoy, "Acoustic Diffraction Analysis by the Impulse Response Method: A Line Impulse Response Approach," *J. Acoust. Soc. Am.*, vol.76, no.1, pp.280-290, 1984.

[13] N. Denisenko, G. Scarano, M. Matteucci and M. Pappalardo, "An Approximate Solution of the Transient Acoustic Field," *IEEE Trans. Son. Ultrason.*, vol.SU-29, no.2, pp.821-827, 1985.

[14] J. Zemanek, "Beam Behavior within the Nearfield of a Vibrating Piston," *J. Acoust. Soc. Am.*, vol.49, no.1, pp.181-191, 1970.

[15] A. Weyns, "Radiation Field Calculations of Pulsed Ultrasonic Transducers: Part I - Planar Circular, Square and Annular Transducers," *Ultrasonics*, pp.183-188, 1980.

[16] A. Weyns, "Radiation Field Calculations of Pulsed Ultrasonic Transducers: Part II - Spherical Disc- and Ring-Shaped Transducers," *Ultrasonics*, pp.219-223, 1980.

[17] R. Lerch and W. Friedrich, "Ultrasound Fields in Atteuating Media," *J. Acoust. Soc. Am.*, vol.80, no.4, pp.1140-1147, 1986.

[18] J. W. Goodman, *Introduction to Fourier Optics*, McGraw-Hill, New York,1968.

[19] P. M. Morse and K. U. Ingard, *Theoretical Acoustics*, McGraw-Hill, New York, 1968, Chap. 7.

[20] K. B. Ocheltree and L. A. Frizzell, "Sound Field Calculation for Rectangular Sources," *IEEE Trans. Ultrason. Ferroelectr. Freq. Contr.*, vol.UFFC-36, no.2, pp.242-248, 1989.

[21] C. K. Lee and P. J. Benkeser, "Computationally Efficient Sound Field Calculations for a Circular Array Transducer," *IEEE Trans. Ultrason. Ferroelectr. Freq. Contr.*, vol.UFFC-39, no.1, pp.43-47, 1992.

Chankil Lee received the B.S degree from the Hanyang University in 1981, the M.S. degree from the Seoul National University in 1983, and the Ph.D. degree from Georgia Institute of Technology in 1992, all in electrical engineering. From 1983 to 1985, he was involved in development of TDX-1 system at ETRI. During 1986-1992, he worked on the radio signal processing and the diffraction problems of acoustic radiators. In 1992, he joined Radio Technology Department at ETRI, where he worked on CDMA mobile radio systems. Currently he is with the Electronic Department of Kyungpook National University, where he teaches and conducts research in radiowave propagation, multipath fading channel characterization, and mobile radio communication.